FGF23 impairs peripheral microvascular function in renal failure

NIGRAM Consortium; Verkaik, Melissa; Juni, Rio P.; van Loon, Ellen P.M.; van Poelgeest, Erik M.; Kwekkeboom, Rick F.J.; Gam, Zeineb; Richards, William G.; Ter Wee, Pieter M.; Hoenderop, Joost G.

Published in:
American Journal of Physiology - Heart and Circulatory Physiology

DOI:
10.1152/ajpheart.00272.2018

Am J Physiol Heart Circ Physiol 315: H1414–H1424, 2018.
First published July 20, 2018; doi:10.1152/ajpheart.00272.2018.

RESEARCH ARTICLE | *Vascular Biology and Microcirculation*

FGF23 impairs peripheral microvascular function in renal failure

Melissa Verkaik,[1] Rio P. Juni,[2] Ellen P. M. van Loon,[3] Erik M. van Poelgeest,[3] Rick F. J. Kwekkeboom,[2] Zeineb Gam,[2] William G. Richards,[4] Pieter M. ter Wee,[1] Joost G. Hoenderop,[3] Etto C. Eringa,[2]* Marc G. Vervloet,[1]* and the NIGRAM Consortium

[1]*Department of Nephrology and Institute for Cardiovascular Research VU, VU University Medical Center, Amsterdam, The Netherlands;* [2]*Department of Physiology, Institute for Cardiovascular Research VU, VU University Medical Center, Amsterdam, The Netherlands;* [3]*Department of Physiology, Radboud Institute for Molecular Life Sciences, Radboud University Medical Center, Nijmegen, The Netherlands; and* [4]*Amgen Incorporated, Thousand Oaks, California*

Submitted 30 April 2018; accepted in final form 18 July 2018

Verkaik M, Juni RP, van Loon EP, van Poelgeest EM, Kwekkeboom RF, Gam Z, Richards WG, ter Wee PM, Hoenderop JG, Eringa EC, Vervloet MG; NIGRAM Consortium. FGF23 impairs peripheral microvascular function in renal failure. *Am J Physiol Heart Circ Physiol* 315: H1414–H1424, 2018. First published July 20, 2018; doi:10.1152/ajpheart.00272.2018.—Cardiovascular diseases account for ~50% of mortality in patients with chronic kidney disease (CKD). Fibroblast growth factor 23 (FGF23) is independently associated with endothelial dysfunction and cardiovascular mortality. We hypothesized that CKD impairs microvascular endothelial function and that this can be attributed to FGF23. Mice were subjected to partial nephrectomy (5/6Nx) or sham surgery. To evaluate the functional role of FGF23, non-CKD mice received FGF23 injections and CKD mice received FGF23-blocking antibodies after 5/6Nx surgery. To examine microvascular function, myocardial perfusion in vivo and vascular function of gracilis resistance arteries ex vivo were assessed in mice. 5/6Nx surgery blunted ex vivo vasodilator responses to acetylcholine, whereas responses to sodium nitroprusside or endothelin were normal. In vivo FGF23 injections in non-CKD mice mimicked this endothelial defect, and FGF23 antibodies in 5/6Nx mice prevented endothelial dysfunction. Stimulation of microvascular endothelial cells with FGF23 in vitro did not induce ERK phosphorylation. Increased plasma asymmetric dimethylarginine concentrations were increased by FGF23 and strongly correlated with endothelial dysfunction. Increased FGF23 concentration did not mimic impaired endothelial function in the myocardium of 5/6Nx mice. In conclusion, impaired peripheral endothelium-dependent vasodilatation in 5/6Nx mice is mediated by FGF23 and can be prevented by blocking FGF23. These data corroborate FGF23 as an important target to combat cardiovascular disease in CKD.

NEW & NOTEWORTHY In the present study, we provide the first evidence that fibroblast growth factor 23 (FGF23) is a cause of peripheral endothelial dysfunction in a model of early chronic kidney disease (CKD) and that endothelial dysfunction in CKD can be prevented by blockade of FGF23. This pathological effect on endothelial cells was induced by long-term exposure of physiological levels of FGF23. Mechanistically, increased plasma asymmetric dimethylarginine concentrations were strongly associated with this endothelial dysfunction in CKD and were increased by FGF23.

CKD-MBD; endothelial dysfunction; FGF23; microcirculation; nitric oxide

INTRODUCTION

Chronic kidney disease (CKD) is a major public health problem worldwide with a prevalence of ~10% in the United Kingdom population and 14% in the United States population (7, 45a). Of note, patients with CKD frequently die because of cardiovascular complications before reaching end-stage renal disease (39). In those progressing to end-stage renal disease, an additional 50% also die from cardiovascular disease.

When correcting for classical cardiovascular risk factors commonly seen in patients with CKD, renal failure itself remains an important risk factor for cardiovascular events (20). This suggests that other features of CKD contribute to the increased cardiovascular risk. In patients with CKD, nontraditional risk factors for cardiovascular diseases, like activation of the renin-angiotensin system, endothelial dysfunction, oxidative stress, and inflammation, frequently coincide. Fibroblast growth factor 23 (FGF23) has emerged as an additional potent biomarker for cardiovascular risk in patients with CKD, and besides being a predictor of all-cause and cardiovascular mortality, it has also been associated with CKD progression. Interestingly, a causal role of FGF23 in the development of left ventricular (LV) hypertrophy (LVH) has been suggested (16). Several epidemiological studies have demonstrated strong associations between increased FGF23 concentration and LV mass (21, 33), which was corroborated by the study by Faul et al. (16) showing that FGF23 directly induces hypertrophy of cardiomyocytes. Interestingly, FGF23 was also linked to impaired LV function, even in the absence of LVH (41), but mechanistic data are lacking on how FGF23 might affect cardiac function independent from LVH induction.

A possible link between increased plasma FGF23 concentration and cardiac dysfunction might be an abnormal vascular function, which is frequently observed in patients with CKD. Under pathophysiological conditions, vasodilator reserve in resistance arteries in the myocardium is decreased, consequently limiting perfusion reserve of the coronary microcirculation, contributing to heart failure (29, 53). In addition, peripheral vascular dysfunction predicts the occurrence of cardiovascular events (5), suggesting these two vascular abnormalities develop in parallel. Serum FGF23 concentrations are associated with in-

* E. C. Eringa and M. G. Vervloet contributed equally to this work.
Address for reprint requests and other correspondence: M. G. Vervloet, De Boelelaan 1117, Room 0D12, Amsterdam 1081HV, The Netherlands (e-mail: m.vervloet@vumc.nl).

creased arterial stiffness and impaired vasoreactivity in both experimental animal models or renal failure and patients with CKD (32, 43, 50, 51).

In the present study, we tested the hypothesis that FGF23 directly impairs vascular function in CKD and whether this can be restored by blocking FGF23 effects. To this end, we used the gracilis artery of mice, which is a model resistance artery to study regulation of microvascular perfusion and resistance. In addition, vascular function in the heart was studied by visualizing and quantifying myocardial perfusion with myocardial contrast echocardiography (MCE).

MATERIALS AND METHODS

Animals. All male C57BL/6 mice (Charles River Laboratories, Leiden, The Netherlands) were housed under standardized conditions and received water and food ad libitum. Chow diet (TD.2016, 0.7% P_i) was provided to all animals unless mentioned otherwise. All mice were placed into individual metabolic cages (Tecniplast, Milan, Italy) at the end of the study period for the collection of 24-h urine samples. All experiments were approved and conducted following guidelines of the local animal ethical committee at the VU University Medical Center (Amsterdam, The Netherlands) and complied with Dutch government guidelines.

Induction of CKD. Seven-week-old mice were subjected to either 5/6 nephrectomy (5/6Nx), as previously described (10), or sham surgery under isoflurane anesthesia and preoperative analgesia (buprenorphine, Temgesic, Schering-Plough, 0.05 mg/kg im; Fig. 1*A*). An abdominal dorsal midline incision was made, and the left kidney was decapsulated, after which the upper and lower poles were removed by a bipolar electrocoagulator. In the same procedure, the complete decapsulated right kidney was removed after ligation of the renal blood vessels and the ureter. After surgery, all mice received subcutaneous injections of postoperative analgesia for 2 consecutive days (ketoprofen, Ketofen, Merial, 5 mg/kg). In control mice, sham surgery was performed, which included decapsulation of both kidneys but no removal of kidney tissue. The rest of the protocol was followed as described above. Six weeks after surgery, cardiovascular function was examined.

Exogenous FGF23 supplementation. Thirteen-week-old mice were injected intraperitoneally twice daily for 7 consecutive days with either vehicle (PBS) or 160 $\mu g \cdot kg^{-1} \cdot day^{-1}$ recombinant mouse FGF23 (8 μg/ml, R&D Systems, Minneapolis, MN, degradation resistant; Fig. 1*B*) (14). After 7 days, cardiovascular function was examined.

Intraperitoneal injections with FGF23 antibodies. To determine the effective dose of anti-rat monoclonal FGF23 antibodies (kindly provided by Amgen, Thousand Oaks, CA), 7-wk-old mice were subjected to 5/6Nx, recovered for 2 wk, and received a single intraperitoneal injection with either rat isotype control antibody (IgG_{2a}), 3 mg/kg FGF23 antibody, 10 mg/kg FGF23, or 30 mg/kg FGF23 antibody. Blood was taken before surgery, before injection, and 9, 24, and 48 h after injection, and plasma phosphate concentration was measured.

Seven-week-old mice were subjected to 5/6Nx, as described above, and received either rat isotype control antibodies (IgG_{2a}, 10 mg/kg) with normal phosphate diet (TD.2016, 0.7% P_i) or received anti-rat FGF23 monoclonal antibodies (10 mg/kg) with a low-phosphate diet (TD.01582, 0.2% P_i) to avoid the development of hyperphosphatemia (Fig. 1*C*). The first antibody suspension was given on the day of surgery and was repeated with intraperitoneal injections (10 ml/kg) every 48 h for the remainder of the study. Six weeks after surgery, cardiovascular function was examined.

CKD-related parameters, electrolytes, FGF23, and asymmetric dimethylarginine in plasma. Blood was centrifuged for 10 min at 3,000 rpm at 4°C, and plasma samples were stored at −80°C. Urea, creatinine, and phosphate concentrations from EDTA-anticoagulated plasma were determined by in-hospital services using automatic

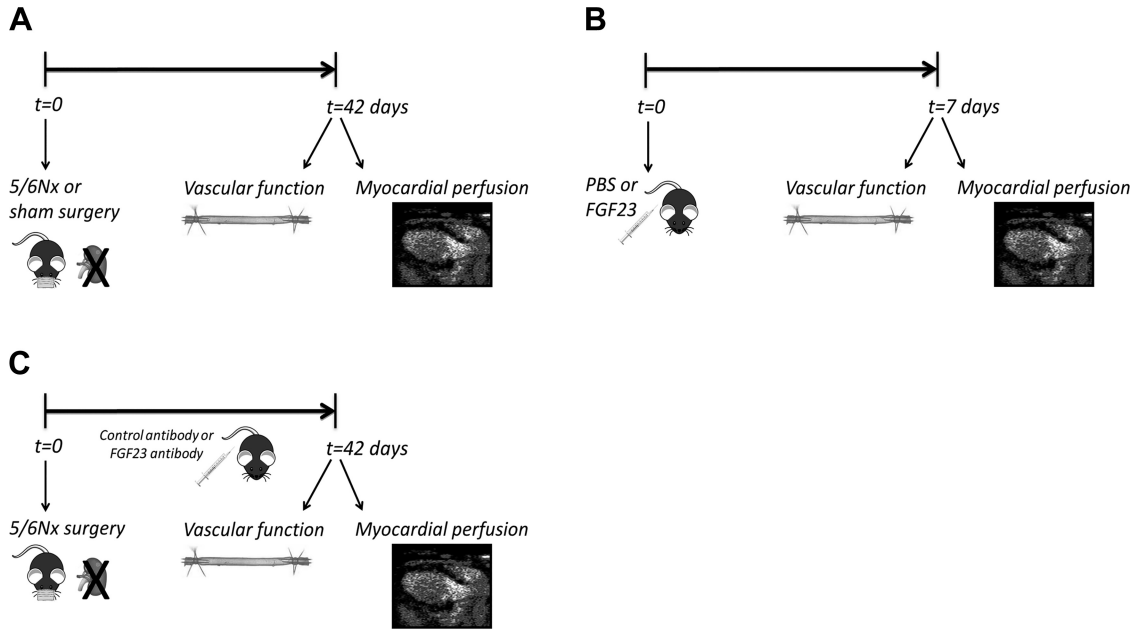

Fig. 1. Mouse models used to assess vascular function and myocardial perfusion. *A*: 7-wk-old male C57BL/6 mice were subjected to either sham surgery or 5/6 nephrectomy (5/6Nx) surgery. After 42 days, vascular function and myocardial perfusion were assessed. *B*: 13-wk-old male C57BL/6 mice were injected intraperitoneally twice daily for 7 consecutive days with either vehicle (PBS) or 160 $\mu g \cdot kg^{-1} \cdot day^{-1}$ recombinant mouse fibroblast growth factor 23 (FGF23; 8 μg/ml). After 7 days, vascular function and myocardial perfusion were assessed. *C*: 7-wk-old male C57BL/6 mice were subjected to 5/6Nx surgery and received either control antibodies (10 mg/kg) with normal phosphate diet or received anti-FGF23-blocking antibodies (10 mg/kg) with a low-phosphate diet. The first antibody suspension was given on the day of surgery and repeated with intraperitoneal injections every 48 h for the remainder of the study. After 42 days, vascular function and myocardial perfusion were assessed.

biochemical analyzers. Ca^{2+} concentrations from heparin-anticoagulated plasma or urine samples were determined using a commercial serum standard (Precinorm U, Roche) and measured as previously described (36). Circulating c-term FGF23 concentrations from EDTA-anticoagulated plasma were measured in duplicate using a rodent-specific ELISA (Immutopics, San Clemente, CA) according to the manufacturer's protocol. Asymmetric dimethylarginine (ADMA) was measured by a novel ELISA (DLD, Diagnostika, Hamburg, Germany) (40).

Ex vivo vascular function experiments. Vasoreactivity of resistance arteries was characterized ex vivo in resistance arteries isolated from the gracilis muscle of mice as previously described (30). In brief, after dissection of the gracilis artery, arteries were placed into a pressure myograph containing MOPS buffer that consisted of 145 mmol/l NaCl, 4.7 mmol/l KCl, 2.5 mmol/l $CaCl_2$, 1.0 mmol/l $MgSO_4$, 1.2 mmol/l NaH_2PO_4, 2.0 mmol/l pyruvate, 0.02 mmol/l EDTA, 3.0 mmol/l MOPS, 5.5 mmol/l glucose, and 0.1% BSA at pH 7.4, after which the diameter was monitored continuously. Arteries were incubated for 45 min with KCl (25 mmol/l) to induce vasoconstriction. Acute effects of acetylcholine on endothelium-dependent vasodilatation of the gracilis artery were studied at five different concentrations (ranging from 10^{-9} to 10^{-5} mol/l). Acute effects of sodium nitroprusside (SNP) on endothelium-independent vasodilatation were studied at six different concentrations (ranging from 10^{-9} to 10^{-4} mol/l). Finally, acute effects of endothelin (Sigma-Aldrich, St. Louis, MO) on endothelium-independent vasoconstriction were studied at five different concentrations (from 10^{-11} to 10^{-7} mol/l). To determine the acute effects of a high dose of FGF23 on endothelial function, 10 ng/ml FGF23 (catalog no. 2629-FG-025/CF, R&D Systems) was added to the pressure myograph 1 h before the first acetylcholine application.

Myocardial perfusion measurements. To evaluate the effects of CKD on myocardial perfusion, mice were anesthetized with intraperitoneal injections of fentanyl, midazolam, and acepromazine. A venous line was placed in the jugular vein for the infusion of both microbubbles (for ultrasound contrast) and vasodilators. MCE was performed with a Siemens-Acuson Sequoia 512 with a 17L5 transducer (Siemens-Acuson, Mountain View, CA), as previously described (37). In brief, microbubble were generated by a combination of 1,2-distearoyl-*sn*-glycero-3-phosphocholine (DSPC; Avanti Polar Lipids) and polyoxyethylene stearate (PEG40, Sigma) at a molecular ratio of 3:1 and were solved in a 0.9% saline-glycerol (Life Sciences) mixture (volume: 3:2) in a 2-ml tube with perfluorobutane gas [C4F10(g), F2 Chemicals, Lancashire, UK] in the capspace. Microbubbles were produced by means of mechanical agitation using a VialmixTM (Lantheus Medical Imaging, North Billerica, MA) high-speed shaker. Subsequently, microbubble size distribution and concentration were determined using a Multisizer 3 (Beckman Coulter Nederland, Woerden, The Netherlands), after which microbubbles were diluted in saline to a final concentration of 1×10^9 microbubbles/ml. Microbubbles were infused at a rate of 7.5 μl/min for 2 min to reach a systemic steady state. Four real-time inflow curves of >10 s each in a long-axis view of the heart in the end-systolic phase of the cardiac cycle were recorded after destruction of the microbubbles by a sequence of eight high-energy pulses (mechanical index of 1.7). Thirty minutes after baseline measurements were acquired, acetylcholine (5 $\mu g \cdot kg^{-1} \cdot min^{-1}$, 15 mg/l) was infused intravenously to assess myocardial blood flow reserve. After 5 min of continuous infusion of the vasodilator and 2 min infusion of microbubbles, four real-time inflow curves were obtained as described above. Microbubble inflow curves were analyzed offline using the Image Processing toolbox in MATLAB (MathWorks, Natick, MA). Average intensity was measured in a region of interest, which was manually drawn on the myocardial wall of the LV. No corrections had to be made, since microbubble concentrations were equal across all mice and measurements. Video intensities within the region of interest were then fitted to the following exponential function: $y = A(1-e^{-\beta t})$, where y is the signal video intensity at any given time, A is the plateau video intensity representing the microvascular blood volume, β is the initial slope of the curve representing microvascular filling velocity, and t is the time after the start of the inflow curve.

Measurement of arterial blood pressure. After the induction of anesthesia, the left carotid artery was cannulated, and arterial blood pressure was continuously recorded using PowerLab software (PowerLab 8/35, Chart 7.0, AD Instruments). Mean arterial blood pressure was calculated after the induction of anesthesia but before MCE.

In vitro effects of FGF23 on human microvascular endothelial cells. This study was executed in accordance with the Declaration of Helsinki and was approved by the Medical Ethics Committee of the VU University Medical Center. Human microvascular endothelial cells (MVECs) were isolated from the foreskin (kindly provided by the Department of Dermatology), cultured, and characterized (CD31, *von Willebrand factor*, *Ulex europaeus* lectin-1 binding, and vascular-endothelial cadherin) as previously described (46, 47). In brief, pooled human MVECs (*passage 6*) from 13 donors were cultured on 1% gelatin-coated culture plates in endothelial growth medium (EGM)-2MV (CC-3203, Lonza) at 37°C in a 5% CO_2-95% air atmosphere. Upon confluency, cells were treated with culture medium without human FGF2 (CC-4147, Lonza) for 24 h as a positive control for FGF receptor (FGFR)1 activation. Cells were then treated with culture medium without human FGF2 or with 4 ng/ml human FGF2 or 10 nM recombinant human FGF23 (no. 2604-FG, R&D Systems) for 30 min. Subsequently, the culture medium was discarded, and whole cell lysates were obtained by scraping the cells in the presence of ice-cold 2× SDS sample buffer. Protein samples were loaded onto 8% SDS gels, electrophoresed, and transferred to nitrocellulose membranes. Protein analysis was performed by incubation of the nitrocellulose membranes with primary antibody against phospho-ERK1/2 (1:500, no. 9106S, Cell Signaling Technology). Blots were then stripped and incubated with primary antibody against total ERK1/2 (1:1,000, no. 9102, Cell Signaling Technology). Protein bands were visualized using enhanced chemiluminescence (Amersham/GE Healthcare) on an AI600 machine (Amersham/GE Healthcare), and bands of both ERK1 and ERK2 were analyzed.

Determination of endothelial nitric oxide synthase coupling. Low-temperature SDS-PAGE and Western blot analysis were performed for the detection of endothelial nitric oxide (NO) synthase (eNOS) dimers as previously described (49). Briefly, total proteins of femoral arteries of all groups were separated by 6% SDS-PAGE. Electrophoresis was performed at 4°C. Proteins were transferred to PVDF membranes, which were probed with an eNOS antibody (ab5589, Abcam). Immunoreactive bands were detected with an appropriate second antibody and visualized with a chemiluminescence kit (GE Healthcare). α-Actinine was used as a loading control.

Statistics. Data are presented as means ± SE. The number of mice in individual experiments is shown in the figures. Differences between groups were assessed by a Mann-Whitney test and within groups by a Wilcoxon test. The correlation between ADMA and maximum response upon acetylcholine and between ADMA and FGF23 concentrations was analyzed by linear regression. For ex vivo vascular function analysis, linear mixed models were used to test whether the relation between relative increase (outcome/dependent variable) and the vasoactive substance concentration (acetylcholine, SNP, or endothelin) differed between groups. The mixed models included a random intercept for mice and fixed effects for groups, vasoactive substance concentration level indicator, and their interaction. Main interest was in testing the interaction between groups and vasoactive substance concentration. If the interaction was not significant, the interaction was removed from the model, and the main effect of groups was considered to see if groups differed in the relative increase (averaged over the concentrations). Two-tailed P values of <0.05 were considered statistically significant. Outliers were removed from data sets when samples were more than three times the interquartile range. Tests were performed using SPSS version 22.

RESULTS

5/6Nx surgery increases plasma FGF23 concentration. 5/6Nx surgery induced renal impairment as reflected by increased plasma urea and creatinine concentration 6 wk after surgery compared with sham controls (Table 1). The volume of urine production was approximately five times higher in 5/6Nx mice compared with sham mice 6 wk after surgery (0.4 ± 0.1 vs. 1.8 ± 0.2 ml/24 h, $P < 0.001$; Table 2). No significant difference in plasma phosphate concentration was observed between groups (Table 1). In contrast, urinary phosphate concentration was approximately six times higher and fractional excretion of phosphate was approximately four times higher in 5/6Nx mice compared with sham mice. Compared with sham surgery, 5/6Nx surgery caused a statistically significant 1.5-fold increase in plasma c-term FGF23 concentration (Table 1).

FGF23 antibodies administered to 5/6Nx mice or FGF23 intraperitoneal injections in isolation did not change urea or creatinine concentrations in plasma and urine (Table 3). As a consequence of the low-phosphate diet, the plasma phosphate concentration increased only slightly in 5/6Nx mice that received control antibodies compared with FGF23 antibodies (2.66 ± 0.12 vs. 2.32 ± 0.09 mmol/l, respectively, $P = 0.043$; Table 3), and urinary phosphate excretion was approximately five times lower in 5/6Nx mice that received FGF23 antibodies (96.11 ± 2.43 vs. 21.18 ± 1.81 μmol/24 h, $P = 0.007$; Table 3).

Both CKD and exogenous FGF23 impair endothelium-dependent vasodilatation but not vascular smooth muscle cell relaxation. Resistance arteries from 5/6Nx mice showed attenuated endothelium-dependent vasodilation upon acetylcholine compared with sham mice ($P < 0.05$), indicating endothelial dysfunction (Fig. 2*A*). At all tested concentrations of acetylcholine (10^{-9}–10^{-5} mol/l), vasodilator responses of the gracilis artery were attenuated compared with sham mice. In addition, the maximum response to acetylcholine was decreased (84.2% vs. 54.8%, $P = 0.003$; data not shown). In both control groups, i.e., sham surgery and PBS intraperitoneal injections, a similar response to acetylcholine was observed. In turn, FGF23 intraperitoneal injections blunted the vasodilatory response upon acetylcholine comparable to 5/6Nx mice ($P < 0.05$; Fig. 2*A*). Acute exposure to recombinant FGF23 (1 h) of gracilis arteries from sham and 5/6Nx mice showed no difference in the response to acetylcholine (Fig. 2*D*). Vascular responses to SNP and endothelin showed no difference between control and intervention groups (Fig. 2, *B* and *C*).

FGF23 blockade restores endothelial function in mice with CKD. The optimal dose of FGF23 antibody was determined by a single intraperitoneal injection with different concentrations 2 wk after 5/6Nx surgery. Injection with 10 or 30 mg/kg FGF23 antibody increased plasma phosphate concentration to the same extent, and it continued to be increased up to 48 h (Fig. 3). Plasma phosphate concentration after injection with control antibody or 3 mg/kg FGF23 antibody did not change over time (Fig. 3). Based on these pilot data, a dose of 10 mg/kg was chosen for subsequent experiments, which was repeated every 48 h.

Mice that received FGF23 antibodies after 5/6Nx surgery showed restored arteriolar vasodilatory capacity upon incremental concentrations of acetylcholine compared with 5/6Nx mice that received control antibodies ($P = 0.048$; Fig. 4*A*). SNP and endothelin did not show a different vascular response between 5/6Nx mice that received control or FGF23 antibodies ($P = 0.445$ for SNP and $P = 0.552$ for endothelin; Fig. 4, *B* and *C*).

FGF23 stimulation does not induce signal transduction in MVECs. MVECs were stimulated with vehicle (negative control), FGF2 (positive control), or FGF23 for 30 min, and total and phosphorylated ERK protein expression was measured (Fig. 5*A*). FGF2 stimulation increased ERK phosphorylation compared with vehicle (1.95 ± 0.24 vs. 1.00 ± 0.19, $P = 0.0159$, respectively), whereas FGF23 stimulation did not increase ERK phosphorylation in MVECs compared with vehicle (0.95 ± 0.19 vs. 1.00 ± 0.19, respectively; Fig. 5*B*).

Endothelial dysfunction is associated with increased concentrations of ADMA and is not caused by eNOS uncoupling. 5/6Nx surgery and FGF23 antibody treatment in 5/6Nx mice did not change plasma ADMA concentrations compared with sham surgery or control antibody treatment ($P = 0.372$ and $P = 0.116$, respectively; Fig. 6*A*). Recombinant FGF23 signif-

Table 1. *5/6Nximpairs kidney function and increases plasma FGF23 concentration*

	Sham	5/6Nx
Plasma urea, mmol/l	12.7 ± 0.3	22.1 ± 1.1‡
Plasma creatinine, μmol/l	15.0 ± 1.5	28.3 ± 1.6‡
Urinary creatinine, μmol/24 h	2.62 ± 0.23	3.33 ± 0.15*
Creatinine clearance, μl/min	137.1 ± 20.4	92.8 ± 6.0
Plasma P_i, mmol/l	3.37 ± 0.19	2.93 ± 0.12
Urinary P_i, μmol/24 h	19.2 ± 2.8	115.0 ± 18.4‡
FEP, %	2.95 ± 0.92	17.01 ± 2.87†
Plasma c-term FGF23, pg/ml	210.2 ± 13.1	315.2 ± 27.6†
Plasma Ca^{2+}, mmol/l	2.00 ± 0.02	2.17 ± 0.03‡
Urinary Ca^{2+}, μmol/24 h	1.07 ± 0.21	3.55 ± 0.31‡
Plasma 1,25-dihydroxyvitamin D_3, pmol/l	226.8 ± 10.2	252.6 ± 23.5
Plasma parathyroid hormone, pg/ml	255.6 ± 51.8	555.4 ± 83.8*

Data are means ± SE. $n = 9$–14 for sham except for fractional excretion of phosphate (FEP), fibroblast growth factor 23 (FGF23), and vitamin D, where $n = 6$; and $n = 18$–21 for 5/6Nx except for creatinine clearance, FEP, FGF23, and vitamin D, where $n = 16$, $n = 15$, $n = 16$, and $n = 7$, respectively. Renal parameters of mice subjected to sham or 5/6Nx surgery are shown. Urinary parameters were calculated from urine (Table 2). *$P \leq 0.05$; †$P \leq 0.01$; ‡$P \leq 0.001$ vs. sham, by Mann-Whitney test.

Table 2. *Effects of induced chronic kidney disease, FGF23 antibodies, and increased FGF23 concentrations on general physiological parameters*

	Body weight, g	Food intake, g/24 h	Water intake, ml/24 h	Urine output, ml/24 h
Sham	26.8 ± 0.4	2.5 ± 0.1	3.0 ± 0.2	0.4 ± 0.1
5/6Nx	25.4 ± 0.4*	2.8 ± 0.2	5.3 ± 0.5‡	1.8 ± 0.2‡
5/6Nx + control antibody	23.3 ± 0.2	2.8 ± 0.1	5.2 ± 0.2	2.2 ± 0.3
5/6Nx + FGF23 antibody	25.3 ± 0.5†	2.2 ± 0.3	3.9 ± 0.9	1.6 ± 0.4
PBS injections	27.5 ± 1.2	2.4 ± 0.3	2.4 ± 0.4	0.7 ± 0.1
FGF23 injections	28.1 ± 1.0	1.7 ± 0.2	2.2 ± 0.4	1.0 ± 0.1

Data are means ± SE; $n = 13$–14 for sham, $n = 19$–20 for 5/6 nephrectomy (5/6Nx), $n = 8$–9 for 5/6Nx + control antibody, $n = 8$–9 for 5/6Nx + fibroblast growth factor 23 (FGF23) antibody, $n = 7$ for PBS injections, and $n = 8$ for FGF23 injections. Body weight, food intake, water intake, and urine output of mice subjected to sham or 5/6Nx surgery, control or FGF23 antibody after 5/6Nx, and PBS or FGF23 intraperitoneal injections are shown. *$P \leq 0.05$; †$P \leq 0.01$; ‡$P \leq 0.001$ compared with the matching control group, i.e., sham, 5/6Nx + control antibody, or PBS injections.

Table 3. *FGF23 antibodies in 5/6Nx mice alter phosphate concentration but not FGF23 injections in isolation*

	PBS	FGF23	Control Antibody	FGF23 Antibody
Plasma urea, mmol/l	8.4 ± 0.4	7.6 ± 0.2	23.2 ± 1.7	21.3 ± 1.0
Plasma creatinine, μmol/l	9.4 ± 0.9	8.4 ± 0.6	28.2 ± 2.0	21.9 ± 1.3
Urinary creatinine, μmol/24 h	2.97 ± 0.64	3.81 ± 0.36	3.61 ± 0.29	3.33 ± 0.30
Plasma P_i, mmol/l	1.61 ± 0.06	1.61 ± 0.08	2.66 ± 0.12	2.32 ± 0.09*
Urinary P_i, μmol/24 h	68.93 ± 12.67	86.76 ± 6.09	96.11 ± 2.43	21.18 ± 1.81†

Data are mean ± SE; n = 5–7 for PBS, n = 7–8 for fibroblast growth factor 23 (FGF23), n = 4–6 for control antibody except for urinary creatinine, where n = 9, and n = 4–5 and n = 8–9 for FGF23 antibody for plasma and urine parameters, respectively. Renal parameters of mice subjected to PBS or FGF23 intraperitoneal injections and of 5/6 nephrectomy (5/6Nx) mice that received control or FGF23 antibody. Plasma was collected at the end of the experiment. Urinary parameters were calculated from 24-h urine. *$P \leq 0.05$; †$P \leq 0.01$ compared with control antibody.

icantly increased ADMA concentrations compared with vehicle (PBS) injections (0.96 ± 0.05 vs. 0.83 ± 0.05 μmol/l, respectively, P = 0.046). A strong correlation was observed for a decreased acetylcholine response of the gracilis artery with increased plasma ADMA concentrations in 5/6Nx mice (R^2 = 0.65, P = 0.0029; Fig. 6*B*).

eNOS uncoupling occurs when the eNOS dimeric form shifts to a monomeric form. Monomer protein expression of

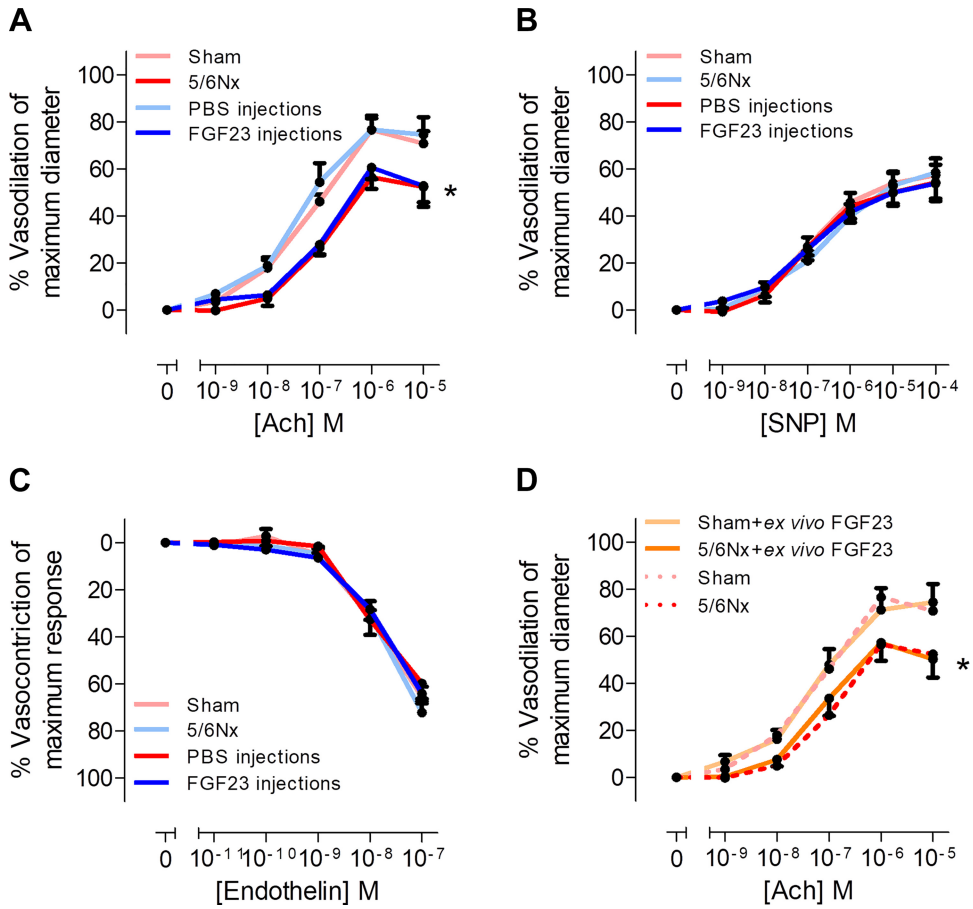

Fig. 2. 5/6 Nephrectomy (5/6Nx) impairs endothelial but not vascular smooth muscle function, which is mimicked by chronically increasing circulating fibroblast growth factor 23 (FGF23) concentration. *A*: 5/6Nx attenuated endothelium-dependent vasodilator responses of the gracilis artery, and this effect was mimicked by increasing FGF23 intraperitoneal injections. The pink line shows sham surgery (n = 12), the light blue line shows PBS intraperitoneal injections (n = 8), the red line shows 5/6Nx surgery (n = 8), and the dark blue line shows FGF23 intraperitoneal injections (n = 7). *B*: 5/6Nx and increased FGF23 concentration in isolation did not impair vasodilator responses of gracilis resistance arteries to the endothelium-independent vasodilator sodium nitroprusside (SNP). The pink line shows sham surgery (n = 9), the light blue line shows PBS intraperitoneal injections (n = 8), the red line shows 5/6Nx surgery (n = 8), and the dark blue line shows FGF23 intraperitoneal injections (n = 7). *C*: 5/6Nx and high concentration of FGF23 in the absence of chronic kidney disease do not impair vasoconstrictor responses to endothelin. The pink line shows sham surgery (n = 6), the light blue line shows PBS intraperitoneal injections (n = 5), the red line shows 5/6Nx surgery (n = 5), and the dark blue line shows FGF23 intraperitoneal injections (n = 7). *D*: arteries from sham and 5/6Nx mice were incubated for 1 h with recombinant FGF23 and subsequently exposed to acetylcholine (ACh), but this did not change endothelial function compared with arteries without incubation with FGF23. The light orange line shows sham surgery and ex vivo FGF23 incubation (n = 7), the dark orange line shows 5/6Nx surgery and ex vivo FGF23 incubation (n = 7), the pink dotted line shows sham surgery (n = 12), and the red dotted line shows 5/6Nx surgery (n = 8). Data are means ± SE. *$P \leq 0.05$ vs. sham or PBS, by linear mixed models.

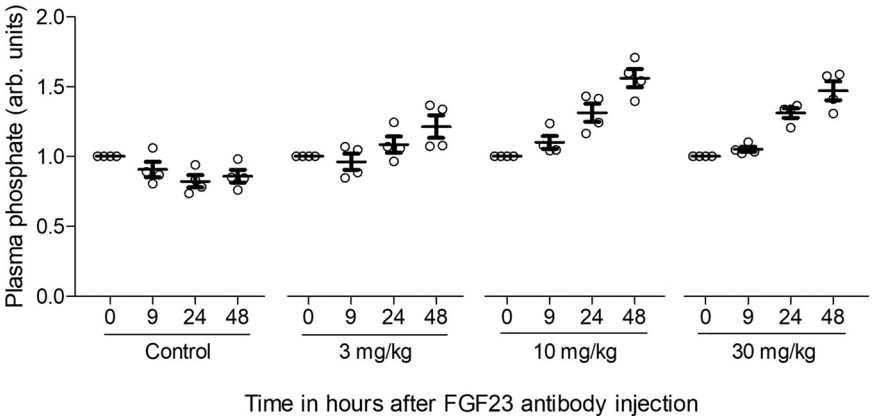

Fig. 3. Fibroblast growth factor 23 (FGF23) blockade increases plasma phosphate in 5/6 nephrectomized (5/6Nx) mice. Plasma phosphate concentrations before 5/6Nx surgery (−2 wk), before a single dose injection (0), and 9, 24, and 48 h after injection are shown. Plasma phosphate did not increase after injection with control antibody or after 3 mg/kg FGF23 antibody injection. After a single dose injection with 10 mg/kg FGF23 antibodies, plasma phosphate increased up to 48 h after injection. The same trend was seen for 30 mg/kg FGF23 antibody injection. $n = 4$ per group. Data are means ± SE.

eNOS in femoral arteries was not detected in sham and 5/6Nx mice, PBS- and FGF23-injected mice, or in 5/6Nx mice that received control or FGF23 antibodies (Fig. 7).

FGF23 does not explain the disturbed vasodilation in CKD of the myocardial microcirculation. Mean arterial blood pressure was not different between sham and 5/6Nx mice (77.8 ± 4.2 and 71.1 ± 5.2 mmHg, respectively; Fig. 8*A*). Acetylcholine increased myocardial microvascular blood volume in sham mice by 52% ($P = 0.002$ vs. baseline; Fig. 8*B*) and in 5/6Nx mice by 28% ($P = 0.040$ vs. baseline). The difference in microvascular blood volume after acetylcholine infusion between groups did not reach statistical significance ($P = 0.068$). Both groups that received PBS intraperitoneal injections or FGF23 intraperitoneal injections increased their myocardial blood volume upon acetylcholine infusion by 83% and 74%, respectively ($P = 0.005$ for both groups compared with baseline; Fig. 8*B*), but no difference was observed between groups. 5/6Nx mice that received control antibodies increased their myocardial microvascular blood volume upon acetylcholine by 47% ($P = 0.017$ vs. baseline; Fig. 8*B*), and 5/6Nx mice that received FGF23 antibodies increased their microvascular blood volume by 28% ($P = 0.043$ vs. baseline). No difference between groups in the response to acetylcholine was detected.

The heart weight-to-tibia length ratio was not increased in 5/6Nx mice compared with sham mice (6.34 ± 0.09 vs. 6.16 ± 0.13 mg/mm, respectively; Fig. 8*C*) after 6 wk. Also, FGF23 injections did not induce LVH compared with PBS-

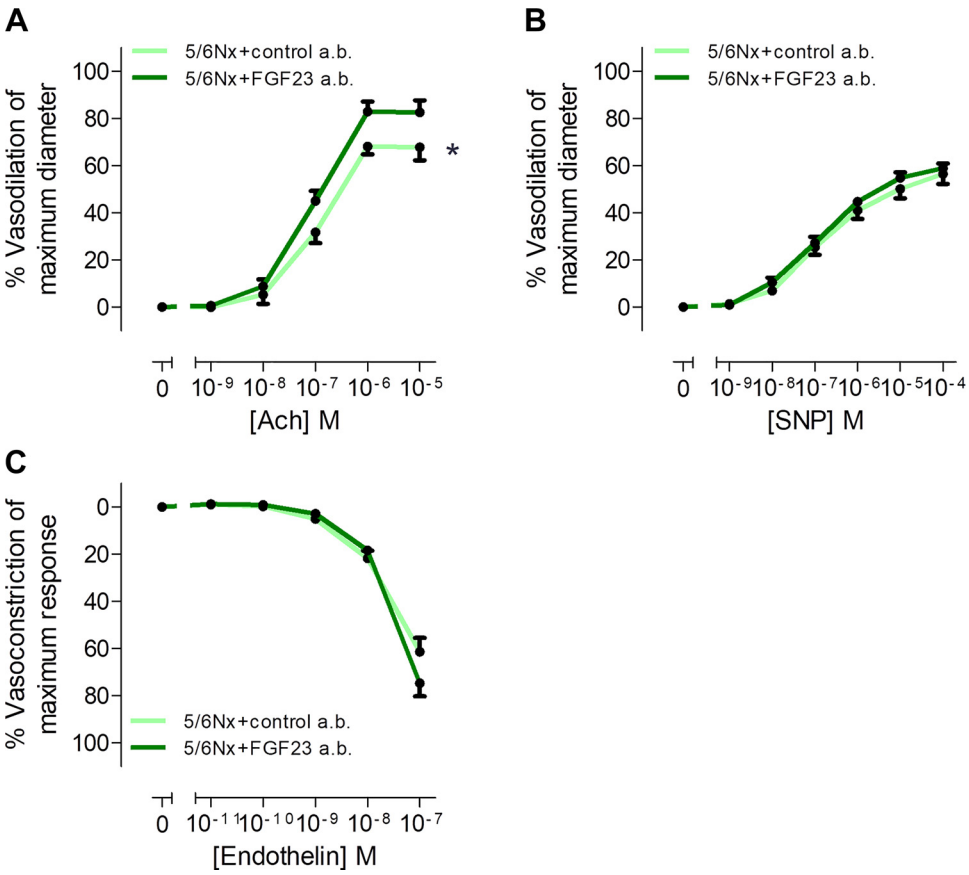

Fig. 4. Fibroblast growth factor 23 (FGF23) blockade normalizes peripheral endothelial function in mice with chronic kidney disease. *A*: FGF23 blockade restored endothelium-dependent vasodilation of the gracilis artery upon acetylcholine (ACh) in mice that underwent 5/6 nephrectomy (5/6Nx) surgery compared with the administration of control antibodies (a.b.). The dark green line shows 5/6Nx surgery with FGF23 antibodies ($n = 8$) and the light green line shows 5/6Nx surgery with control antibodies ($n = 9$). *B*: FGF23 blockade did not restore the vasodilator response of the gracilis artery upon sodium nitroprusside (SNP) in 5/6Nx mice that received control or FGF23 antibodies. The dark green line shows 5/6Nx surgery with FGF23 antibodies ($n = 7$) and the light green line shows 5/6Nx surgery with control antibodies ($n = 8$). *C*: vasoconstrictor response upon endothelin between 5/6Nx mice that received control or FGF23 antibodies. The dark green line shows 5/6Nx surgery with FGF23 antibodies and the light green line shows 5/6Nx surgery with control antibodies. Data are means ± SE. *$P \leq 0.05$ vs. FGF23 antibodies, by linear mixed models.

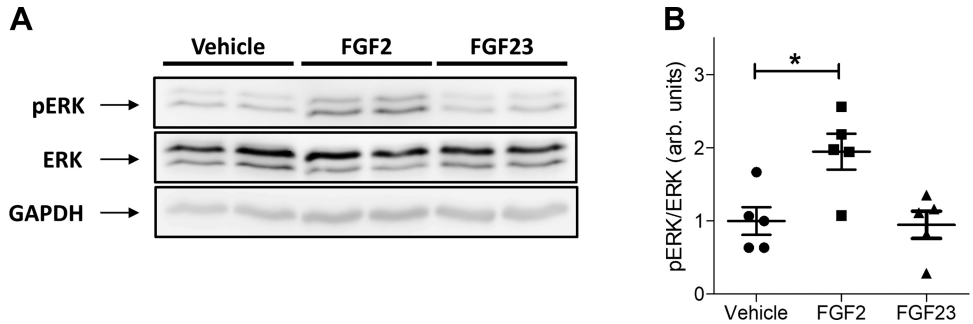

Fig. 5. Fibroblast growth factor (FGF)23 stimulation does not increase ERK phosphorylation in microvascular endothelial cells (MVECs). *A*: MCEVs were stimulated for 30 min with vehicle (negative control), FGF2 (positive control), or FGF23 alone. Total ERK1 and ERK2 (ERK) and phosphorylated ERK1 and ERK2 (pERK) protein expression was quantified by Western blot analysis. *B*: FGF2 significantly ($P = 0.0159$) increased the pERK-to-ERK ratio compared with vehicle, whereas FGF23 did not change the pERK-to-ERK ratio compared with vehicle. Differences between FGF2 and FGF23 stimulation were not significant ($P = 0.0556$). $n = 5$ per stimulation. Data are means ± SE. *$P \leq 0.05$, by Mann-Whitney test.

injected mice (7.07 ± 0.30 vs. 6.86 ± 0.13 mg/mm, respectively; Fig. 8*C*).

DISCUSSION

The main finding of our study is that increased levels of FGF23 cause endothelial dysfunction in peripheral resistance arteries in CKD. FGF23 blockade prevents this pathological effect of FGF23 on endothelial cell function. Mice with CKD also show impaired endothelial function in the myocardium; however, in this vascular bed, increased FGF23 levels could not explain this dysfunction.

Endothelial dysfunction was observed both in mice with CKD and in mice that received exogenous FGF23 in vivo. Vasodilator and contractile vascular smooth muscle cell function was not altered, pointing to a selective endothelial effect of FGF23. The lack of an acute effect of FGF23 on endothelial function in our ex vivo models can have several explanations. First, vascular dysfunction could occur only after long-term exposure to high FGF23 concentrations. Alternatively, the effects of FGF23 are indirect by mechanisms triggered only by in vivo FGF23 exposure (see below). A final explanation may be that circulating factors are required that are absent in the ex vivo setup (11). We did not detect signal transduction in MVECs after FGF23 stimulation, and it therefore may be more likely that our findings are explained by indirect effects of FGF23 through nonendothelial mechanisms or the absence of a cofactor that subsequently interfere with endothelial cell function, as discussed below. Our finding that FGF23 blockade prevents CKD-induced endothelial dysfunction supports a causal role for FGF23 in thedisturbed microcirculation.

Although one study did not demonstrate an effect of FGF23 on endothelium-dependent and endothelium-independent vasodilation (28), another study showed that FGF23 inhibited endothelium-dependent vasodilation ex vivo, yet only at con-

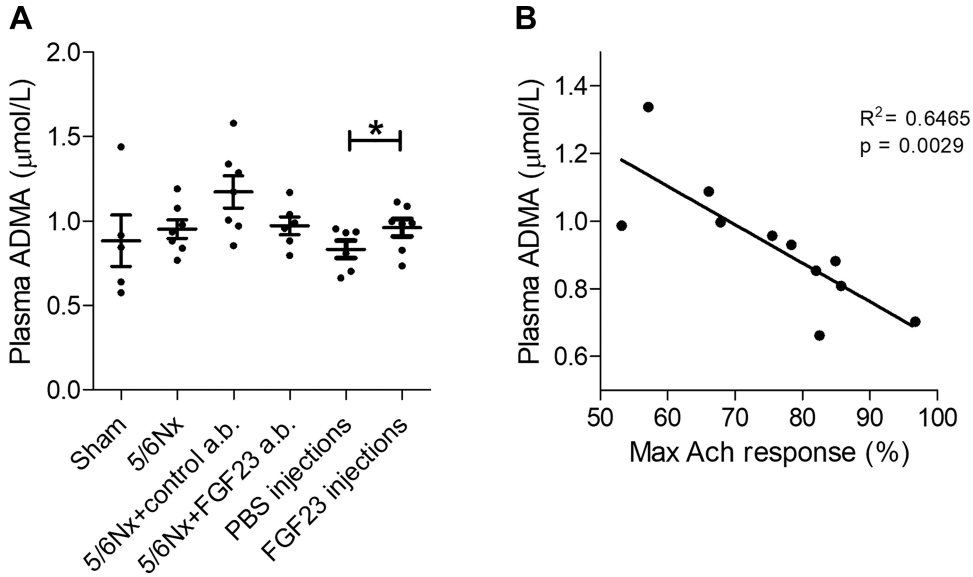

Fig. 6. Asymmetric dimethylarginine (ADMA) is related to fibroblast growth factor 23 (FGF23) concentration in vivo and to the maximal vasodilator response in resistance arteries. *A*: 5/6 nephrectomize (5/6Nx) mice did not increase ADMA plasma concentration compared with sham mice. FGF23 antibodies failed to significantly lower ADMA concentration in 5/6Nx mice, although a clear trend was observed in these mice compared with mice that received control antibodies. Mice injected with recombinant FGF23 significantly increased ADMA concentration compared with PBS-injected mice. $n = 5$ for sham, $n = 7$ for 5/6Nx, FGF23 injections, and 5/6Nx + control antibodies, and $n = 6$ for 5/6Nx + FGF23 antibodies and PBS injections. Data are means ± SE. *$P \leq 0.05$, by Mann-Whitney test. *B*: endothelial function in the gracilis artery was measured ex vivo with acetylcholine (ACh). The maximum response to acetylcholine [Max ACh response (in %)] was inversely related to ADMA concentration ($P = 0.0029$). Linear regression was used for analysis.

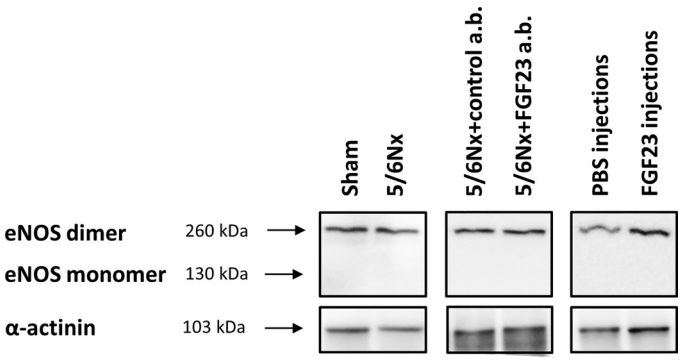

Fig. 7. 5/6 Nephrectomy (5/6Nx) and fibroblast growth factor 23 (FGF23) injections do not induce endothelial nitric oxide synthase (eNOS) monomer protein expression. eNOS protein expression was measured by low-temperature SDS-PAGE to detect both eNOS monomers and dimers. eNOS monomers were not detected after 5/6Nx, 5/6Nx + control antibodies (a.b.), or FGF23 injections, whereas eNOS dimers were present in all groups. $n = 8$ per group except for the 5/6Nx + control antibody group, where $n = 7$.

centrations of 9,000 pg/ml (43). These studies and our results strengthen the hypothesis that acute exposure of physiological concentrations of FGF23 to the vasculature does not impair endothelial function. Silswal et al. (43) showed impaired endothelial function ex vivo in a mouse model with increased FGF23 concentrations, although these FGF23 levels are considered supraphysiological. Our study also showed impaired endothelial function ex vivo, but our 5/6Nx mouse model resulted in FGF23 concentrations seen for this rather mild degree of CKD.

Since we observed only endothelial dysfunction, assessed by acetylcholine, and not vascular smooth muscle dysfunction with elevated circulating FGF23 concentrations, this can only be explained by disturbed NO formation, which is the most important contributor to endothelium-dependent relaxation (15). An important mechanism underlying decreased NO is eNOS uncoupling (19). In the present study, however, we did not observe FGF23-induced eNOS uncoupling as an explanation for disturbed eNOS function but rather increased plasma ADMA levels, which are an important cause of reduced endothelium-dependent vasodilation (42). Moreover, increases in ADMA concentrations have been previously reported in kidney failure (52). In our study, 5/6Nx surgery did not significantly increase plasma ADMA concentrations, although we demonstrated a large variation in sham mice, as such given rise to an unforeseen limited statistical power to detect a difference. FGF23 injections did increase ADMA concentrations, and when FGF23 antibodies were administered to 5/6Nx mice, ADMA tended to decrease. In addition, ADMA was negatively correlated with the maximum response of resistance arteries to acetylcholine, indicating that increased plasma ADMA concentration contributes to the observed endothelial dysfunction in our model of CKD. An association of FGF23 with plasma ADMA concentration has been observed in previous studies (45, 50), strengthening the hypothesis that FGF23-induced endothelial dysfunction is at least partially caused by a decrease of NO bioavailability by ADMA. A recent study even suggested that FGF23 and ADMA act jointly on eNOS (45).

ADMA is released by protein hydrolysis and is eliminated by renal excretion but more so by metabolic degradation by dimethylarginine dimethylaminohydrolases (DDAHs) (35). Inhibition of DDAH is posttranscriptionally regulated by ROS, and oxidative stress in endothelial cells can therefore increase ADMA concentrations. Two recent studies have shown that FGF23 induces ROS production in endothelial cells (38, 43), which could link the increased ADMA levels observed with high FGF23 concentrations. Further research is needed to prove this hypothesis.

A previous study has indicated that peripheral vascular dysfunction predicts the occurrence of cardiovascular events (5). In the present study, in addition to peripheral endothelial dysfunction, we observed a trend for myocardial endothelial dysfunction in our mouse model of early CKD, independent from LVH. Modulation of FGF23 concentrations, however, did not change this microvascular blood volume reserve. This difference in response in vascular beds may be explained by different intrinsic properties of the microvascular beds (3, 4). An alternative explanation for the discrepancy between peripheral and myocardial vascular responses upon increased FGF23 concentrations might be the difference in experimental setup. Whereas peripheral vascular function was measured ex vivo, myocardial perfusion was measured in vivo, and other variables like heart rate, blood pressure, and circulating factors could have influenced the in vivo measurements. Another reason for the discrepancy between endothelial function in different vascular beds might be caused by a different activity of DDAH. It has been shown in previous studies that DDAH activity in the heart is five times higher than in skeletal muscle (13), possibly indicating that the increased FGF23-induced ROS production in these endothelial cells is not sufficient to impair NO production. These results may indicate that also in patients with CKD, endothelial dysfunction in the myocardial vasculature may not be attributed to increased FGF23 concentrations but rather to other uremic toxins.

It is well known that patients suffering from CKD are at an increased risk for cardiovascular events (2, 6, 9, 18, 22, 23, 26, 48). FGF23 has emerged as a potent biomarker for cardiovascular risk in patients with CKD, and several clinical studies have shown a relationship between increased FGF23 concentration and endothelial dysfunction (8, 32, 44, 50, 51). Importantly, clinically even a mild increase of FGF23, in the range of in our present model, is already detrimental (17, 32). In the present study, we show that mice with early CKD develop peripheral endothelial dysfunction, which is explained by increased circulating FGF23 levels. By blocking FGF23, endothelial dysfunction was prevented in this model of early CKD. Lowering FGF23 would therefore qualify as a target in early CKD to combat cardiovascular disease. Indeed, lower serum FGF23 concentrations are associated with lower rates of cardiovascular death and major cardiovascular events, which can be explained by an improved endothelial function (12, 34).

Our study has several limitations. Serum phosphate concentration did not differ between sham and 5/6Nx mice, but urinary phosphate was highly increased. In concert, calcium loss was also higher in 5/6Nx mice (Table 1). Increased circulating parathyroid hormone (PTH) concentrations in our 5/6Nx mouse model might explain the calcium and phosphate imbalance by increased bone turnover. In addition, we cannot exclude that the improved endothelial function in 5/6Nx mice that received FGF23 antibodies is caused by the low-phosphate diet and the subsequent slightly lower plasma phosphate concentration (Table 3).

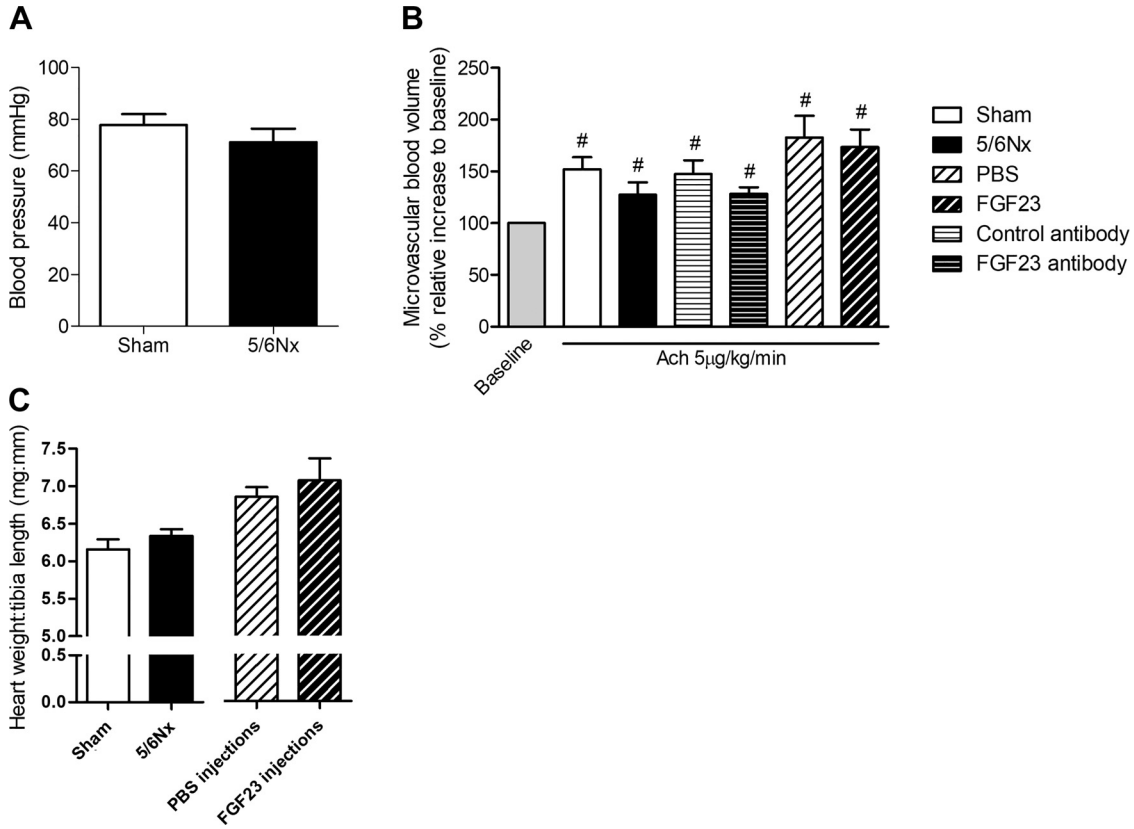

Fig. 8. 5/6 Nephrectomy (5/6Nx) impairs cardiac microvascular blood volume reserve, which is independent from increased fibroblast growth factor 23 (FGF23) concentration and left ventricular hypertrophy. *A*: mean arterial blood pressure was not different 6 wk after sham or 5/6Nx surgery. $n = 5$ for sham and $n = 6$ for 5/6Nx. *B*: all mice significantly increased their microvascular blood volume upon infusion of the endothelium-dependent vasodilator acetylcholine (ACh; 5 $\mu g \cdot kg^{-1} \cdot min^{-1}$) compared with baseline. Increments in 5/6Nx mice were lower compared with sham mice, although not significant ($P = 0.068$). $n = 13$ for sham mice, $n = 17$ for 5/6Nx mice, $n = 10$ for 5/6Nx mice that received control antibodies, $n = 5$ for 5/6Nx mice that received FGF23 antibodies, $n = 10$ for PBS-injected mice, and $n = 11$ for FGF23-injected mice. *C*: the heart weight-to-tibia length ratio was not increased in 5/6Nx mice compared with sham mice (6.34 ± 0.09 vs. 6.16 ± 0.13 mg/mm, respectively) 6 wk after surgery. Also, the heart weight-to-tibia length ratio was not different between mice that received PBS injections or FGF23 injections (6.86 ± 0.13 vs. 7.07 ± 0.30 mg/mm, respectively). $n = 11$ for sham mice, $n = 16$ for 5/6Nx mice, $n = 15$ for PBS-injected mice, and $n = 13$ for FGF23-injected mice. Data are means ± SE. #$P \leq 0.05$ vs. baseline and *$P \leq 0.05$ vs. 5/6Nx, by Mann-Whitney test between groups and Wilcoxon test within groups.

We did not study the potential effects of FGF23 on endothelial cells by other FGF receptors than subtype 1. However, no study to date has demonstrated FGF23 effects mediated by FGFR2, FGFR3, or FGFR4 on endothelial cells. A study by Lim et al. (27) has demonstrated FGF23 signal transduction by ERK phosphorylation in vascular cells, but depending on the presence of Klotho and FGFR1. Richter et al. (38) also found Klotho-dependent activation of FGFR1 by FGF23 in endothelial cells, resulting in Akt phosphorylation. Here, we assessed ERK signal transduction, and we therefore cannot exclude that Akt phosphorylation was induced. However, ERK phosphorylation would have been expected after FGF2 signal transduction mediated by FGFR1. Extensive studies from our group, however, have refuted the presence of functional Klotho in the vasculature (31).

We cannot exclude that in our ex vivo and in vitro setup the lack of soluble Klotho in the medium caused an absence of FGF23-induced signal transduction in vascular endothelial cells. A recent study has shown that transmembrane or shed Klotho is required for receptor activation, and future studies on FGF23 function should therefore include soluble Klotho in ex vivo and in vitro experimental setups (11).

Consistent with our results, others found that C57BL/6 mice that underwent 5/6Nx are resistant to blood pressure increases and progression of renal disease (24, 25). Although the lack of progressive kidney disease or development of LVH in the rodent model we used is paradoxical, we did demonstrate that the effects of FGF23 on the microcirculation in mice differ for different vascular beds. Species differences therefore may account for differences in development of end-organ damage. In addition, an important difference with clinical CKD is the duration of exposure to uremia and elevated FGF23 concentration. Also, it is possible that in clinical CKD, the additional burden of hypertension, superimposed on uremia and elevated FGF23, is mandatory for end-organ damage. For our model, however, the lack of hypertension mitigates potential confounding effects of superimposed hypertension and strengthens the likelihood that observed abnormalities were endocrine, i.e., FGF23, and not hemodynamic in origin. The lack of hypertension, LVH, or progression of renal disease in C57BL/6 mice implies that microvascular dysfunction, induced by increased FGF23 concentrations, is an early step in the development of cardiovascular disease in CKD.

Although ex vivo vascular function was assessed in the gracilis artery, tissue was too small to measure eNOS expression. The larger femoral artery was chosen, of which the gracilis artery is a side branch, as this is anatomically close to the gracilis artery.

In conclusion, our study shows that increased FGF23 concentrations cause peripheral endothelial dysfunction in a model of early CKD and that FGF23 blockade can be beneficial to combat cardiovascular disease in CKD.

ACKNOWLEDGMENTS

The NIGRAM consortium consists of the following principal investigators: Piet ter Wee, Marc Vervloet (VU University Medical Center, Amsterdam, The Netherlands), René Bindels, Joost Hoenderop (Radboud University Medical Center, Nijmegen, The Netherlands), Gerjan Navis, Jan-Luuk Hillebrands, and Martin de Borst (University Medical Center Groningen, Groningen, The Netherlands).

GRANTS

This work was supported by Dutch Kidney Foundation Consortium Grant NIGRAM CP10.11. J. Hoenderop is supported by The Netherlands Organization for Scientific Research Grant 016.130.668. E. C. Eringa is supported by The Netherlands Organization for Scientific Research Grant 016.136.372. M. G. Vervloet received research funding from Dutch Kidney Foundation Grants CP10.11, 13.OI.06, and 15.OP.02.

DISCLOSURES

W. G. Richards is employed by Amgen and as such receives salary and stock from Amgen and owns Amgen stock. M. G. Vervloet received research funding from AbbVie and Amgen. M. Verkaik was, in part, paid by contract research funding by Amgen. None of the other authors has any conflicts of interest, financial or otherwise, to disclose.

AUTHOR CONTRIBUTIONS

M.V., W.G.R., P.M.t.W., J.G.H., E.C.E., and M.G.V. conceived and designed research; M.V., R.P.J., E.P.v.L., E.v.P., R.F.K., and Z.G. performed experiments; M.V., R.P.J., E.P.v.L., E.v.P., and Z.G. analyzed data; M.V., R.P.J., E.P.v.L., R.F.K., Z.G., W.G.R., P.M.t.W., J.G.H., E.C.E., and M.G.V. interpreted results of experiments; M.V., R.P.J., and Z.G. prepared figures; M.V. drafted manuscript; M.V., E.C.E., and M.G.V. edited and revised manuscript; M.V., R.P.J., E.P.v.L., E.v.P., R.F.K., Z.G., W.G.R., P.M.t.W., J.G.H., E.C.E., and M.G.V. approved final version of manuscript.

REFERENCES

2. **Abramson JL, Jurkovitz CT, Vaccarino V, Weintraub WS, McClellan W.** Chronic kidney disease, anemia, and incident stroke in a middle-aged, community-based population: the ARIC Study. *Kidney Int* 64: 610–615, 2003. doi:10.1046/j.1523-1755.2003.00109.x.
3. **Aird WC.** Phenotypic heterogeneity of the endothelium: I. Structure, function, and mechanisms. *Circ Res* 100: 158–173, 2007. doi:10.1161/01.RES.0000255691.76142.4a.
4. **Aird WC.** Phenotypic heterogeneity of the endothelium: II. Representative vascular beds. *Circ Res* 100: 174–190, 2007. doi:10.1161/01.RES.0000255690.03436.ae.
5. **Akiyama E, Sugiyama S, Matsuzawa Y, Konishi M, Suzuki H, Nozaki T, Ohba K, Matsubara J, Maeda H, Horibata Y, Sakamoto K, Sugamura K, Yamamuro M, Sumida H, Kaikita K, Iwashita S, Matsui K, Kimura K, Umemura S, Ogawa H.** Incremental prognostic significance of peripheral endothelial dysfunction in patients with heart failure with normal left ventricular ejection fraction. *J Am Coll Cardiol* 60: 1778–1786, 2012. doi:10.1016/j.jacc.2012.07.036.
6. **Alonso A, Lopez FL, Matsushita K, Loehr LR, Agarwal SK, Chen LY, Soliman EZ, Astor BC, Coresh J.** Chronic kidney disease is associated with the incidence of atrial fibrillation: the Atherosclerosis Risk in Communities (ARIC) study. *Circulation* 123: 2946–2953, 2011. doi:10.1161/CIRCULATIONAHA.111.020982.
7. **Archibald G, Bartlett W, Brown A, Christie B, Elliott A, Griffith K, Pound S, Rappaport I, Robertson D, Semple Y, Slane P, Whitworth C, Williams B.** UK Consensus Conference on Early Chronic Kidney Disease−6 and 7 February 2007. *Nephrol Dial Transplant* 22: 2455–2457, 2007. doi:10.1093/ndt/gfm268.
8. **Ärnlöv J, Carlsson AC, Sundström J, Ingelsson E, Larsson A, Lind L, Larsson TE.** Serum FGF23 and risk of cardiovascular events in relation to mineral metabolism and cardiovascular pathology. *Clin J Am Soc Nephrol* 8: 781–786, 2013. doi:10.2215/CJN.09570912.
9. **Astor BC, Coresh J, Heiss G, Pettitt D, Sarnak MJ.** Kidney function and anemia as risk factors for coronary heart disease and mortality: the Atherosclerosis Risk in Communities (ARIC) Study. *Am Heart J* 151: 492–500, 2006. doi:10.1016/j.ahj.2005.03.055.
10. **Bro S, Bentzon JF, Falk E, Andersen CB, Olgaard K, Nielsen LB.** Chronic renal failure accelerates atherogenesis in apolipoprotein E-deficient mice. *J Am Soc Nephrol* 14: 2466–2474, 2003. doi:10.1097/01.ASN.0000088024.72216.2E.
11. **Chen G, Liu Y, Goetz R, Fu L, Jayaraman S, Hu MC, Moe OW, Liang G, Li X, Mohammadi M.** α-Klotho is a non-enzymatic molecular scaffold for FGF23 hormone signalling. *Nature* 553: 461–466, 2018. doi:10.1038/nature25451.
12. **Choi SR, Lim JH, Kim MY, Hong YA, Chung BH, Chung S, Choi BS, Yang CW, Kim YS, Chang YS, Park CW.** Cinacalcet improves endothelial dysfunction and cardiac hypertrophy in patients on hemodialysis with secondary hyperparathyroidism. *Nephron Clin Pract* 122: 1–8, 2012. doi:10.1159/000347145.
13. **Davids M, Richir MC, Visser M, Ellger B, van den Berghe G, van Leeuwen PA, Teerlink T.** Role of dimethylarginine dimethylaminohydrolase activity in regulation of tissue and plasma concentrations of asymmetric dimethylarginine in an animal model of prolonged critical illness. *Metabolism* 61: 482–490, 2012. doi:10.1016/j.metabol.2011.08.007.
14. **de Jong MA, Mirkovic K, Mencke R, Hoenderop JG, Bindels RJ, Vervloet MG, Hillebrands JL, van den Born J, Navis G, de Borst MH.** Fibroblast growth factor 23 modifies the pharmacological effects of angiotensin receptor blockade in experimental renal fibrosis. *Nephrol Dial Transplant* 32: 73–80, 2017. doi:10.1093/ndt/gfw105.
15. **Deanfield JE, Halcox JP, Rabelink TJ.** Endothelial function and dysfunction: testing and clinical relevance. *Circulation* 115: 1285–1295, 2007. doi:10.1161/CIRCULATIONAHA.106.652859.
16. **Faul C, Amaral AP, Oskouei B, Hu MC, Sloan A, Isakova T, Gutiérrez OM, Aguillon-Prada R, Lincoln J, Hare JM, Mundel P, Morales A, Scialla J, Fischer M, Soliman EZ, Chen J, Go AS, Rosas SE, Nessel L, Townsend RR, Feldman HI, St John Sutton M, Ojo A, Gadegbeku C, Di Marco GS, Reuter S, Kentrup D, Tiemann K, Brand M, Hill JA, Moe OW, Kuro-o M, Kusek JW, Keane MG, Wolf M.** FGF23 induces left ventricular hypertrophy. *J Clin Invest* 121: 4393–4408, 2011. doi:10.1172/JCI46122.
17. **Fliser D, Kollerits B, Neyer U, Ankerst DP, Lhotta K, Lingenhel A, Ritz E, Kronenberg F; MMKD Study Group.** Fibroblast growth factor 23 (FGF23) predicts progression of chronic kidney disease: the Mild to Moderate Kidney Disease (MMKD) Study. *J Am Soc Nephrol* 18: 2600–2608, 2007. doi:10.1681/ASN.2006080936.
18. **Foley RN, Murray AM, Li S, Herzog CA, McBean AM, Eggers PW, Collins AJ.** Chronic kidney disease and the risk for cardiovascular disease, renal replacement, and death in the United States Medicare population, 1998 to 1999. *J Am Soc Nephrol* 16: 489–495, 2005. doi:10.1681/ASN.2004030203.
19. **Förstermann U, Münzel T.** Endothelial nitric oxide synthase in vascular disease: from marvel to menace. *Circulation* 113: 1708–1714, 2006. doi:10.1161/CIRCULATIONAHA.105.602532.
20. **Go AS, Chertow GM, Fan D, McCulloch CE, Hsu CY.** Chronic kidney disease and the risks of death, cardiovascular events, and hospitalization. *N Engl J Med* 351: 1296–1305, 2004. doi:10.1056/NEJMoa041031.
21. **Gutiérrez OM, Januzzi JL, Isakova T, Laliberte K, Smith K, Collerone G, Sarwar A, Hoffmann U, Coglianese E, Christenson R, Wang TJ, deFilippi C, Wolf M.** Fibroblast growth factor 23 and left ventricular hypertrophy in chronic kidney disease. *Circulation* 119: 2545–2552, 2009. doi:10.1161/CIRCULATIONAHA.108.844506.
22. **Keith DS, Nichols GA, Gullion CM, Brown JB, Smith DH.** Longitudinal follow-up and outcomes among a population with chronic kidney disease in a large managed care organization. *Arch Intern Med* 164: 659–663, 2004. doi:10.1001/archinte.164.6.659.
23. **Kottgen A, Russell SD, Loehr LR, Crainiceanu CM, Rosamond WD, Chang PP, Chambless LE, Coresh J.** Reduced kidney function as a risk factor for incident heart failure: the atherosclerosis risk in communities

(ARIC) study. *J Am Soc Nephrol* 18: 1307–1315, 2007. doi:10.1681/ASN.2006101159.

24. **Kren S, Hostetter TH.** The course of the remnant kidney model in mice. *Kidney Int* 56: 333–337, 1999. doi:10.1046/j.1523-1755.1999.00527.x.
25. **Leelahavanichkul A, Yan Q, Hu X, Eisner C, Huang Y, Chen R, Mizel D, Zhou H, Wright EC, Kopp JB, Schnermann J, Yuen PS, Star RA.** Angiotensin II overcomes strain-dependent resistance of rapid CKD progression in a new remnant kidney mouse model. *Kidney Int* 78: 1136–1153, 2010. doi:10.1038/ki.2010.287.
26. **Levin A, Singer J, Thompson CR, Ross H, Lewis M.** Prevalent left ventricular hypertrophy in the predialysis population: identifying opportunities for intervention. *Am J Kidney Dis* 27: 347–354, 1996. doi:10.1016/S0272-6386(96)90357-1.
27. **Lim K, Lu TS, Molostvov G, Lee C, Lam FT, Zehnder D, Hsiao LL.** Vascular Klotho deficiency potentiates the development of human artery calcification and mediates resistance to fibroblast growth factor 23. *Circulation* 125: 2243–2255, 2012. doi:10.1161/CIRCULATIONAHA.111.053405.
28. **Lindberg K, Olauson H, Amin R, Ponnusamy A, Goetz R, Taylor RF, Mohammadi M, Canfield A, Kublickiene K, Larsson TE.** Arterial klotho expression and FGF23 effects on vascular calcification and function. *PLoS One* 8: e60658, 2013. doi:10.1371/journal.pone.0060658.
29. **Lund GK, Watzinger N, Saeed M, Reddy GP, Yang M, Araoz PA, Curatola D, Bedigian M, Higgins CB.** Chronic heart failure: global left ventricular perfusion and coronary flow reserve with velocity-encoded cine MR imaging: initial results. *Radiology* 227: 209–215, 2003. doi:10.1148/radiol.2271012156.
30. **Meijer RI, Bakker W, Alta CL, Sipkema P, Yudkin JS, Viollet B, Richter EA, Smulders YM, van Hinsbergh VW, Serné EH, Eringa EC.** Perivascular adipose tissue control of insulin-induced vasoreactivity in muscle is impaired in *db*/*db* mice. *Diabetes* 62: 590–598, 2013. doi:10.2337/db11-1603.
31. **Mencke R, Harms G, Mirković K, Struik J, Van Ark J, Van Loon E, Verkaik M, De Borst MH, Zeebregts CJ, Hoenderop JG, Vervloet MG, Hillebrands JL; NIGRAM Consortium.** Membrane-bound Klotho is not expressed endogenously in healthy or uraemic human vascular tissue. *Cardiovasc Res* 108: 220–231, 2015. doi:10.1093/cvr/cvv187.
32. **Mirza MA, Larsson A, Lind L, Larsson TE.** Circulating fibroblast growth factor-23 is associated with vascular dysfunction in the community. *Atherosclerosis* 205: 385–390, 2009. doi:10.1016/j.atherosclerosis.2009.01.001.
33. **Mirza MA, Larsson A, Melhus H, Lind L, Larsson TE.** Serum intact FGF23 associate with left ventricular mass, hypertrophy and geometry in an elderly population. *Atherosclerosis* 207: 546–551, 2009. doi:10.1016/j.atherosclerosis.2009.05.013.
34. **Moe SM, Chertow GM, Parfrey PS, Kubo Y, Block GA, Correa-Rotter R, Drüeke TB, Herzog CA, London GM, Mahaffey KW, Wheeler DC, Stolina M, Dehmel B, Goodman WG, Floege J; Evaluation of Cinacalcet HCl Therapy to Lower Cardiovascular Events (EVOLVE) Trial Investigators.** Cinacalcet, fibroblast growth factor-23, and cardiovascular disease in hemodialysis: the Evaluation of Cinacalcet HCl Therapy to Lower Cardiovascular Events (EVOLVE) Trial. *Circulation* 132: 27–39, 2015. doi:10.1161/CIRCULATIONAHA.114.013876.
35. **Palm F, Onozato ML, Luo Z, Wilcox CS.** Dimethylarginine dimethylaminohydrolase (DDAH): expression, regulation, and function in the cardiovascular and renal systems. *Am J Physiol Heart Circ Physiol* 293: H3227–H3245, 2007. doi:10.1152/ajpheart.00998.2007.
36. **Pulskens WP, Verkaik M, Sheedfar F, van Loon EP, van de Sluis B, Vervloet MG, Hoenderop JG, Bindels RJ; NIGRAM Consortium.** Deregulated renal calcium and phosphate transport during experimental kidney failure. *PLoS One* 10: e0142510, 2015. doi:10.1371/journal.pone.0142510.
37. **Raher MJ, Thibault H, Poh KK, Liu R, Halpern EF, Derumeaux G, Ichinose F, Zapol WM, Bloch KD, Picard MH, Scherrer-Crosbie M.** In vivo characterization of murine myocardial perfusion with myocardial contrast echocardiography: validation and application in nitric oxide synthase 3 deficient mice. *Circulation* 116: 1250–1257, 2007. doi:10.1161/CIRCULATIONAHA.107.707737.
38. **Richter B, Haller J, Haffner D, Leifheit-Nestler M.** Klotho modulates FGF23-mediated NO synthesis and oxidative stress in human coronary artery endothelial cells. *Pflugers Arch* 468: 1621–1635, 2016. doi:10.1007/s00424-016-1858-x.
39. **Schiffrin EL, Lipman ML, Mann JF.** Chronic kidney disease: effects on the cardiovascular system. *Circulation* 116: 85–97, 2007. doi:10.1161/CIRCULATIONAHA.106.678342.
40. **Schulze F, Wesemann R, Schwedhelm E, Sydow K, Albsmeier J, Cooke JP, Böger RH.** Determination of asymmetric dimethylarginine (ADMA) using a novel ELISA assay. *Clin Chem Lab Med* 42: 1377–1383, 2004. doi:10.1515/CCLM.2004.257.
41. **Seiler S, Cremers B, Rebling NM, Hornof F, Jeken J, Kersting S, Steimle C, Ege P, Fehrenz M, Rogacev KS, Scheller B, Böhm M, Fliser D, Heine GH.** The phosphatonin fibroblast growth factor 23 links calcium-phosphate metabolism with left-ventricular dysfunction and atrial fibrillation. *Eur Heart J* 32: 2688–2696, 2011. doi:10.1093/eurheartj/ehr215.
42. **Sibal L, Agarwal SC, Home PD, Boger RH.** The role of asymmetric dimethylarginine (ADMA) in endothelial dysfunction and cardiovascular disease. *Curr Cardiol Rev* 6: 82–90, 2010. doi:10.2174/157340310791162659.
43. **Silswal N, Touchberry CD, Daniel DR, McCarthy DL, Zhang S, Andresen J, Stubbs JR, Wacker MJ.** FGF23 directly impairs endothelium-dependent vasorelaxation by increasing superoxide levels and reducing nitric oxide bioavailability. *Am J Physiol Endocrinol Metab* 307: E426–E436, 2014. doi:10.1152/ajpendo.00264.2014.
44. **Six I, Okazaki H, Gross P, Cagnard J, Boudot C, Maizel J, Drueke TB, Massy ZA.** Direct, acute effects of Klotho and FGF23 on vascular smooth muscle and endothelium. *PLoS One* 9: e93423, 2014. doi:10.1371/journal.pone.0093423.
45. **Tripepi G, Kollerits B, Leonardis D, Yilmaz MI, Postorino M, Fliser D, Mallamaci F, Kronenberg F, Zoccali C.** Competitive interaction between fibroblast growth factor 23 and asymmetric dimethylarginine in patients with CKD. *J Am Soc Nephrol* 26: 935–944, 2015. doi:10.1681/ASN.2013121355.

45a. **U.S. Renal Data System.** *USRDS 2013 Annual Data Report: Atlas of Chronic Kidney Disease and End-Stage Renal Disease in the United States*. Bethesda, MD: National Institutes of Health, National Institute of Diabetes and Digestive and Kidney Diseases, 2013.

46. **van der Heijden M, van Nieuw Amerongen GP, van Bezu J, Paul MA, Groeneveld AB, van Hinsbergh VW.** Opposing effects of the angiopoietins on the thrombin-induced permeability of human pulmonary microvascular endothelial cells. *PLoS One* 6: e23448, 2011. doi:10.1371/journal.pone.0023448.
47. **Van Hinsbergh VW, Sprengers ED, Kooistra T.** Effect of thrombin on the production of plasminogen activators and PA inhibitor-1 by human foreskin microvascular endothelial cells. *Thromb Haemost* 57: 148–153, 1987.
48. **Wattanakit K, Folsom AR, Selvin E, Coresh J, Hirsch AT, Weatherley BD.** Kidney function and risk of peripheral arterial disease: results from the Atherosclerosis Risk in Communities (ARIC) Study. *J Am Soc Nephrol* 18: 629–636, 2007. doi:10.1681/ASN.2005111204.
49. **Yang YM, Huang A, Kaley G, Sun D.** eNOS uncoupling and endothelial dysfunction in aged vessels. *Am J Physiol Heart Circ Physiol* 297: H1829–H1836, 2009. doi:10.1152/ajpheart.00230.2009.
50. **Yilmaz MI, Sonmez A, Saglam M, Yaman H, Kilic S, Demirkaya E, Eyileten T, Caglar K, Oguz Y, Vural A, Yenicesu M, Zoccali C.** FGF-23 and vascular dysfunction in patients with stage 3 and 4 chronic kidney disease. *Kidney Int* 78: 679–685, 2010. doi:10.1038/ki.2010.194.
51. **Yilmaz MI, Sonmez A, Saglam M, Yaman H, Kilic S, Eyileten T, Caglar K, Oguz Y, Vural A, Yenicesu M, Mallamaci F, Zoccali C.** Comparison of calcium acetate and sevelamer on vascular function and fibroblast growth factor 23 in CKD patients: a randomized clinical trial. *Am J Kidney Dis* 59: 177–185, 2012. doi:10.1053/j.ajkd.2011.11.007.
52. **Young JM, Terrin N, Wang X, Greene T, Beck GJ, Kusek JW, Collins AJ, Sarnak MJ, Menon V.** Asymmetric dimethylarginine and mortality in stages 3 to 4 chronic kidney disease. *Clin J Am Soc Nephrol* 4: 1115–1120, 2009. doi:10.2215/CJN.06671208.
53. **Zhang J, Wilke N, Wang Y, Zhang Y, Wang C, Eijgelshoven MH, Cho YK, Murakami Y, Ugurbil K, Bache RJ, From AH.** Functional and bioenergetic consequences of postinfarction left ventricular remodeling in a new porcine model. MRI and ^{31}P-MRS study. *Circulation* 94: 1089–1100, 1996. doi:10.1161/01.CIR.94.5.1089.